Chemical constituents from a marine medicinal brown alga-derived *Xylaria acuta* SC1019

Hsiao-Yang Hsi [a], Shih-Wei Wang [b,c,d], George Hsiao [e,f], Li-Kwan Chang [f], Yuan-Chung Cheng [g], Shu-Jung Huang [a], Yi-Shan Lu [f], Tzong-Huei Lee [a,h,*]

[a] Institute of Fisheries Science, National Taiwan University, Taipei 106, Taiwan
[b] Institute of Biomedical Sciences, MacKay Medical College, New Taipei City 252, Taiwan
[c] Department of Medicine, MacKay Medical College, New Taipei City 252, Taiwan
[d] Graduate Institute of Natural Products, College of Pharmacy, Kaohsiung Medical University, Kaohsiung 807, Taiwan
[e] Department of Pharmacology, School of Medicine, College of Medicine, Taipei Medical University, Taipei 110, Taiwan
[f] Graduate Institute of Medical Sciences, College of Medicine, Taipei Medical University, Taipei 110, Taiwan
[g] Department of Chemistry and Center for Quantum Science and Engineering, National Taiwan University, Taipei 106, Taiwan
[h] Department of Life Science, College of Life Science, National Taiwan University, Taipei 106, Taiwan

Abstract

In this study, a marine medicinal brown alga *Sargassum cristaefolium*-derived fungal strain *Xylaria acuta* SC1019 was isolated and identified. Column chromatography of the extracts from liquid- and solid-fermented products of the fungal strain was carried out, and led to the isolation of twenty-one compounds. Their structures were characterized by spectroscopic analysis, and the absolute configurations were further established by single X-ray diffraction analysis or modified Mosher's method as nine previously undescribed compounds, namely xylarilactones A−C (1−3), *ent*-gedebic acid 8-*O*-α-D-glucopyranoside (4), 5*R*-hydroxylmethylmellein 11-*O*-α-D-glucopyranoside (5), *ent*-hymatoxin E 16-*O*-α-D-mannopyranoside (6), 19,20-epoxycytochalasin S (7), 19,20-epoxycytochalasin T (8), and (2*R*)-butylitaconic acid (9), along with twelve known compounds 10−21. All the isolates were subjected to anti-inflammatory and anti-angiogenic assays. Compounds 1, 5, 7, 10, and 17 showed moderate nitric oxide production inhibitory activities in lipopolysaccharide-activated BV-2 microglial cells with IC_{50} values of 19.55 ± 0.35, 16.10 ± 0.57, 15.20 ± 0.87, 11.76 ± 0.49, and 11.30 ± 0.32 μM, respectively, as compared to curcumin (IC_{50} = 2.69 ± 0.34 μM) without any significant cytotoxicity. Compounds 7, 8, and 21 displayed potent anti-angiogenic activities by suppressing the growth of human endothelial progenitor cells with IC_{50} values of 0.44 ± 0.01, 0.47 ± 0.03, and 0.53 ± 0.01 μM, respectively, as compared to sorafenib (IC_{50} = 5.50 ± 1.50 μM).

Keywords: Anti-angiogenesis, Anti-inflammation, *Xylaria acuta*, Xylariaceae

1. Introduction

Microorganisms from the ocean are renowned for producing secondary metabolites, which possess diverse structures and exhibit unexpected biological properties, making them excellent candidates for pharmaceuticals. So far, our group has published several papers regarding exploratory studies of marine algae-derived fungal metabolites [1,2]. As a component of this ongoing investigation, a marine medicinal brown alga *Sargassum cristaefolium*-derived fungal strain *Xylaria acuta* SC1019 was isolated and identified for the sake of its potentially anti-inflammatory and anti-angiogenic activities in the preliminary screening.

The fungal genus *Xylaria* (Xylariaceae) is the largest genus with more than 300 species reported [3]. Of these, most species were found to be occur as endophytes of plants inducing decay of the white-rot type [4]. To date, more than 450 secondary metabolites, including terpenoids, terpene glycosides, steroids, aromatic compounds, cytochalasin derivatives, and pyranone derivatives, have been reported from this genus [5]. Many of these

Received 14 November 2023; accepted 7 March 2024.
Available online 15 June 2024

* Corresponding author at: Institute of Fisheries Science, National Taiwan University, No.1, Sec. 4, Roosevelt Rd., Taipei 10617, Taiwan.
E-mail address: thlee1@ntu.edu.tw (T.-H. Lee).

https://doi.org/10.38212/2224-6614.3501

compounds exhibited pertinent biological activities for drug exploration, such as cytotoxic [6], antifungal [7], antibacterial [8], and insecticidal [9].

With the aim of pursuing previously undescribed bioactive components from *X. acuta* SC1019, a comprehensive survey involving fungal cultivation, compound separation, structural identification, and bioactivity assessment was carried out. As a result, nine previously unreported chemical entities together with twelve known compounds have been identified. Herein the isolation, characterization, and bioactivities of all the pure isolates were discussed in detail.

2. Materials and methods

2.1. General experimental procedures

Optical rotation, ultraviolet, and IR spectra were measured on a JASCO P-2000 polarimeter (Tokyo, Japan), a Thermo UV−visible Helios α spectrophotometer (Bellefonte, CA, USA), and a JASCO FT/IR 4100 spectrometer (Tokyo, Japan), respectively. ^{1}H and ^{13}C NMR spectra were obtained using an Agilent 600 MHz DD2 NMR spectrometer (Agilent Technologies, Santa Clara, CA, USA). High-resolution electrospray ionization mass spectra were obtained using an Orbitrap QE Plus mass spectrometer MS000100 (Thermo Fisher Scientific Inc., Waltham, MA, USA). Sephadex LH-20 (Sigma−Aldrich, St. Louis, MO, USA) was used for open column chromatography. Thin-layer chromatography was performed using silica gel 60 F_{254} plates (0.2 mm) (Merck, Darmstadt, Germany). X-ray diffraction analysis was measured on a Bruker D8 VENTURE single-crystal XRD (Billerica, Massachusetts, USA) equipped with Oxford Cryostream 800 (Long Hanborough, Oxford, UK). An L-7100 HPLC pump (Hitachi, Tokyo, Japan) equipped with a refractive index detector (Bischoff, Leonberg, Germany) was employed for compound purification.

2.2. Fungal strain isolation and cultivation

The algal material was collected in July, 2021 off the coast of Badouzi (25°08′50.9″N 121°47′42.3″E), Keelung, Taiwan. Algal specimen was identified as *S. cristaefolium* C. Agardh by T.-H.L., one of the authors. A voucher specimen (No. SC-IFS-2021) was deposited at Institute of Fisheries Science, National Taiwan University, Taipei, Taiwan. The alga material was soaked in 75% EtOH followed by 0.01% $NaOCl_{aq}$ and treated with ddH_2O for surface cleaning. The disinfected alga was cut into circles of approximately 5 mm^2. The sample was placed into the seawater PDA (potato dextrose agar) medium and incubated at 28 °C. A single fungal strain was obtained after continuous separation and purification. The mycelium of the fungal strain was lyophilized and ground. The DNA of powdered material was extracted using DNeasy Plant Mini Kit (Qiagen, Venlo, The Netherlands) following the manufacturer's protocol. Two sets of primers ITS4 (forward: 5′-TCCTCCGCTTATTGATATGC-3′) and ITS5 (reverse: 5′-GGAAGTAAAAGTCAAGG-3′) were used to amplify the ITS rRNA. The PCR products were analyzed by Genomic Co., Ltd. (New Taipei City, Taiwan). According to BLAST and phylogenetic analysis based on ITS rDNA gene sequences, the strain was identified as *X. acuta* (No. SC1019). The sequence was deposited in GenBank under the accession number OR229823. This stain is currently preserved in Institute of Fisheries Science, National Taiwan University, Taipei, Taiwan.

2.3. Extraction and isolation of secondary metabolites

Initially, a single colony of *X. acuta* SC1019 from the agar plate was inoculated into the 250 mL flask, each containing 100 mL seawater PDB medium, and incubated at 28 °C for 14 days on a rotary shaker at 180 rpm. Totally, 3.6 L fermentation broth was harvested and partitioned using EtOAc and water for three times. The EtOAc extract (1.9 g) was further subjected to size exclusion chromatography on a Sephadex LH-20 column (3.0 cm i.d. × 68 cm) and eluted with 100% MeOH at a flow rate of 2.0 mL/min to give 25 fractions. Each fraction (25 mL) collected was checked for its composition by TLC using DCM/MeOH (10:1) for development, and dipping in vanillin-H_2SO_4 was used in the detection of compounds with similar skeletons. All fractions were combined into 4 portions PI−PIV. Portion PIII (frs. 9−13) was rechromatographed on a semi-preparative reversed-phase HPLC (Luna® 5 μ PFP 100 Å, 10 × 250 mm) with MeOH/H_2O (1:1, v/v) as eluent at a flow rate of 2.0 mL/min to afford compounds **1** (15.5 mg, t_R = 19.5 min), **2** (7.4 mg, t_R = 32.7 min), **3** (4.2 mg, t_R = 34.4 min), **4** (14.5 mg, t_R = 10.4 min), **5** (5.2 mg, t_R = 12.3 min), **9** (4.0 mg, t_R = 18.7 min), **10** (7.6 mg, t_R = 9.1 min), **11** (5.6 mg, t_R = 14.2 min), **12** (6.7 mg, t_R = 17.1 min), **13** (7.6 mg, t_R = 13.2 min), **14** (10.8 mg, t_R = 55.3 min), **15** (30.3 mg, t_R = 24.3 min), **16** (16.7 mg, t_R = 16.0 min), **17** (31.4 mg, t_R = 17.7 min), and **18** (23.0 mg, t_R = 20.6 min). Compounds **19** (4.6 mg, t_R = 20.0 min) and **20** (14.0 mg, t_R = 13.5 min) was isolated from portion PIV (frs. 14−17) by semi-preparative reversed-phase HPLC (SunFire C18 OBD, 5 μ, 10 × 250 mm) using 50% $MeCN_{aq}$ containing 0.1% formic acid as mobile phase, 2 mL/min.

A single colony of *X. acuta* SC1019 from the agar plate was also used to inoculate into a 250 mL flask, each containing 100 mL seawater ME (malt extract) medium. The fermented mycelia and broth were extracted and fractionationed using the same methods as above. All fractions were combined into 4 portions MI–MIV. Portion MII (frs. 8–12) was rechromatographed on a semi-preparative reversed-phase HPLC (Luna® 5 μ PFP 100 Å, 10 × 250 mm) with MeOH/H_2O (55:45, v/v) as eluent at a flow rate of 2.0 mL/min to afford compound **6** (4.5 mg, t_R = 11.1 min).

In order to obtain varied secondary metabolites, the fungal strain was also grown on a solid medium. Totally, 1.0 kg solid fermented product was harvested and extracted twice with 2 L of MeOH after freeze-drying. The MeOH extract was suspended in H_2O and then partitioned successively with *n*-hexane, EtOAc, and *n*-BuOH for three times to afford *n*-hexane-, EtOAc-, and *n*-BuOH-soluble fractions, respectively. The hexane-soluble fraction (0.39 g) was subjected to size exclusion chromatography on a Sephadex LH-20 column (2.8 cm i.d. × 68 cm) and eluted with 100% MeOH at a flow rate of 2.0 mL/min to give 12 fractions. Each fraction (25 mL) collected was checked for its composition by TLC using DCM/MeOH (10:1) for development, and dipping in vanillin-H_2SO_4 was used in the detection of compounds with similar skeletons. All fractions were combined into 4 portions HI–HIV. Portion HIII (96.3 mg) was separated on semi-preparative HPLC (Synergi™ 4 μm Hydro-RP 80 Å, 10 × 250 mm) with 60% $MeOH_{aq}$ containing 0.1% formic acid as eluent, 2 mL/min, to afford compounds **7** (5.2 mg, t_R = 32.8 min), **8** (18.9 mg, t_R = 22.0 min) and **21** (4.1 mg, t_R = 27.7 min).

2.3.1. *Xylarilactone A (1)*

Amorphous white powder. $[\alpha]_D^{26}$ = 71.4 (*c* 0.1, MeOH); UV (MeOH) λ_{max} (log ϵ) 279 (4.12) nm; IR (ZnSe) υ_{max} 3373, 2931, 1691, 1564, 1456, 1410, 1246, 1022, 823 cm^{-1}; ^1H NMR data see Table 1; ^{13}C NMR data see Table 2; HRESIMS *m/z* 375.1651 $[M + H]^+$ (calcd. 375.1655 for $C_{17}H_{27}O_9$).

2.3.2. *Xylarilactone B (2)*

Colorless oil. $[\alpha]_D^{26}$ = 59.4 (*c* 0.1, MeOH); UV (MeOH) λ_{max} (log ϵ) 278 (4.05) nm; IR (ZnSe) υ_{max} 3371, 2969, 1688, 1563, 1455, 1408, 1245, 1054, 821 cm^{-1}; ^1H NMR data see Table 1; ^{13}C NMR data see Table 2; HRESIMS *m/z* 229.1071 $[M + H]^+$ (calcd. 229.1076 for $C_{11}H_{17}O_5$).

2.3.3. *Xylarilactone C (3)*

Colorless oil. $[\alpha]_D^{26}$ = 67.6 (*c* 0.1, MeOH); UV (MeOH) λ_{max} (log ϵ) 278 (4.05) nm; IR (ZnSe) υ_{max} 3365, 2962, 1688, 1563, 1456, 1408, 1246, 1054, 821 cm^{-1}; ^1H NMR data see Table 1; ^{13}C NMR data see Table 2; HRESIMS *m/z* 229.1071 $[M + H]^+$ (calcd. 229.1076 for $C_{11}H_{17}O_5$).

*Table 1. ^1H and ^{13}C NMR assignments for compounds **1–3** (mult., J in Hz).*

No.	1 [a]		2 [a]		3 [a]	
	δ_C	δ_H	δ_C	δ_H	δ_C	δ_H
2	167.2		167.2		167.2	
3	89.3	5.57 d (2.4)	88.8	5.55 d (1.8)	88.8	5.55 d (1.8)
4	173.7		173.9		173.9	
5	102.0	6.54 dd (0.6, 2.4)	100.1	6.21 dd (0.6, 1.8)	100.1	6.21 dd (0.6, 1.8)
6	165.6		169.0		169.0	
7	75.4	4.52 t (6.0)	71.3	4.35 dd (4.8, 7.8)	71.3	4.35 dd (4.8, 7.8)
8	35.0	1.84 dt (6.0, 7.2)	32.7	1.68 m	32.7	1.78 m
				1.96 m		1.87 m
9	28.6	1.40–1.43 m	35.7	1.47–1.59 m	35.7	1.48–1.59 m
10	23.6	1.34–1.40 m	68.6	3.74 dd (6.6, 12.6)	68.6	3.74 dd (6.0, 12.6)
11	14.3	0.92 t (7.2)	23.6	1.16 d (6.6)	23.6	1.16 d (6.0)
12	57.1	3.87 s	57.1	3.87 s	57.1,	3.87 s
1'	98.3	4.81 d (3.6)				
2'	73.4	3.41 dd (3.6, 9.6)				
3'	74.9	3.68 dd (9.6, 9.6)				
4'	71.9	3.29 dd (9.6, 9.6)				
5'	74.8	3.67 ddd (2.4, 5.4, 9.6)				
6'	62.8	3.68 dd (5.4, 12.0)				
		3.83 dd (2.4, 12.0)				

[a] Data were measured in CD_3OD at 600 MHz for ^1H and 150 MHz for ^{13}C.

*Table 2. ^{1}H and ^{13}C NMR assignments for compounds **4–6** (mult., J in Hz).*

No.	4 [a]		5 [a]		6 [a]	
	δ_C	δ_H	δ_C	δ_H	δ_C	δ_H
1	109.5		171.9		28.6	1.30 m
						1.68 m
2	158.6				19.3	1.55 m
						1.67 m
3	116.9	6.81 d (9.0)	77.5	4.73 qd (6.6, 14.4)	29.7	1.45 dd (7.6, 14.4)
						2.08 ddd (4.8, 7.6, 14.4)
4	127.1	7.50 d (9.0)	32.3	2.92 dd (11.4, 16.8)	44.0	
				3.31, m		
5	147.2		126.8		45.3	2.39 d (4.8)
6	130.7		139.4	7.58 d (8.4)	75.7	4.84 m
7	29.6	2.70 dd (11.4, 17.4)	116.4	6.84 d (8.4)	120.8	5.74 dd (2.4, 4.8)
		3.47 dd (3.6, 17.4)				
8	77.9	4.71 dq (3.6, 6.0)	163.3		146.9	
9	21.2	1.52 d (6.0)	109.7		74.0	
10	171.6		141.5		39.4	
11			67.7	4.54 d (12.0)	27.5	1.53 ddd (3.0, 4.2, 14.4)
				4.71 d (12.0)		1.86 ddd (4.2, 13.2, 14.4)
12			21.1	1.52 d (6.6)	33.6	1.37 m
						1.73 ddd (4.2, 13.2, 13.2)
13					34.6	
14					45.4	2.02 dd (3.0, 15.0)
						2.35 m
15					45.1	1.58 t (6.6)
16					65.2	3.51 td (6.6, 11.4)
						3.88 td (6.6, 11.4)
17					22.6	0.88 s
18					25.3	1.29 s
19					185.9	
20					22.8	0.97 s
1'	101.2	5.34 d (3.6)	99.4	4.84 d (3.6)	101.9	4.73 d (1.8)
2'	73.4	3.58 dd (3.6, 9.6)	73.6	3.40 dd (3.6, 9.6)	72.4	3.77 dd (1.8, 3.6)
3'	75.0	3.81 dd (9.6, 9.6)	75.2	3.64 dd (9.6, 9.6)	72.8	3.67 dd (3.6, 9.6)
4'	71.8	3.39 dd (9.6, 9.6)	72.0	3.27 dd (9.6, 9.6)	68.9	3.59 dd (9.6, 9.6)
5'	75.0	3.70 m	74.2	3.53 ddd (2.4, 6.0, 9.6)	75.0	3.54 ddd (2.4, 6.0, 9.6)
6'	62.7	3.69 m	62.9	3.77 dd (6.0, 11.4)	63.1	3.71 dd (6.0, 11.4)
		3.79 m		3.79 dd (2.4, 11.4)		3.84 dd (2.4, 11.4)

[a] Data were measured in CD_3OD at 600 MHz for ^{1}H and 150 MHz for ^{13}C.

2.3.4. *ent*-gedebic acid 8-O-α-D-glucopyranoside (4)

Amorphous white powder. $[\alpha]_D^{26}$ = 28.0 (*c* 0.1, MeOH); UV (MeOH) λ_{max} (log ϵ) 247 (4.55) and 332 (4.41) nm; IR (ZnSe) υ_{max} 3366, 2929, 1671, 1616, 1515, 1473, 1386, 1212, 1122, 1023, 943 cm^{-1}; ^{1}H NMR data see Table 3; ^{13}C NMR data see Table 4; HRESIMS *m/z* 357.1175 $[M-H_2O + H]^+$ (calcd. 357.1186 for $C_{16}H_{21}O_9$).

2.3.5. 5R-Hydroxylmethylmellein 11-O-α-D-glucopyranoside (5)

Amorphous white powder. $[\alpha]_D^{26}$ = −53.4 (*c* 0.1, MeOH); UV (MeOH) λ_{max} (log ϵ) 249 (4.41) and 317 (3.88) nm; IR (ZnSe) υ_{max} 3365, 2925, 1666, 1604, 1475, 1386, 1218, 1132, 1024 cm^{-1}; ^{1}H NMR data see Table 3; ^{13}C NMR data see Table 4; HRESIMS *m/z* 371.1335 $[M + H]^+$ (calcd. 371.1342 for $C_{17}H_{23}O_9$).

2.3.6. *ent*-hymatoxin E 16-O-α-D-mannopyranoside (6)

Amorphous white powder. $[\alpha]_D^{26}$ = −24.8 (*c* 0.1, MeOH); UV (MeOH) λ_{max} (log ϵ) 250 (3.96) and 255 (3.95) nm; IR (ZnSe) υ_{max} 3367, 2927, 1747, 1596, 1454, 1376, 1203, 1022, 917, 813 cm^{-1}; ^{1}H NMR data see Table 3; ^{13}C NMR data see Table 4; HRESIMS *m/z* $[M-H]^-$ 495.2609 (calcd. 495.2594 for $C_{26}H_{39}O_9$) and *m/z* $[M + H]^+$ 497.2735 (calcd. 497.2751 for $C_{26}H_{41}O_9$).

2.3.7. 19,20-Epoxycytochalasin S (7)

Amorphous white powder. $[\alpha]_D^{26}$ = 24.8 (*c* 0.1, MeOH); UV (MeOH) λ_{max} (log ϵ) 325 (3.76) nm; IR (ZnSe) υ_{max} 3428, 2923, 1743, 1700, 1454, 1369, 1226, 1037, 968 cm^{-1}; ^{1}H NMR and ^{13}C NMR data see Table 5; HRESIMS *m/z* 524.2626 $[M + H]^+$ (calcd. 524.2648 for $C_{30}H_{38}NO_7$).

Table 3. ^1H and ^{13}C NMR assignments for compounds 7–9 (mult., J in Hz).

No.	7 [a]		8 [a]		9 [a]	
	δ_C	δ_H	δ_C	δ_H	δ_C	δ_H
1	176.9		176.8		177.4	
2					48.4	3.44 t (7.8)
3	62.9	3.31 m	56.1	3.63 m	141.3	
4	51.0	2.51 s	51.3	2.20 dd (2.4, 6.0)	169.9	
5	128.1		37.8	1.48 m	32.1	1.68 m 1.85 m
6	134.0		56.6		23.6	1.37 m
7	70.2	3.73 dd (1.2, 10.2)	64.3	2.65 d (5.4)	31.1	1.31 m
8	50.2	2.25 dd (9.6, 10.2)	46.1	2.31 dd (5.4, 10.2)	14.4	0.91 t (7.2)
9	54.1		59.1		126.9	5.74 s 6.31 d (0.6)
10	45.1	3.00 dd (4.8, 13.2) 3.06 dd (10.2, 13.2)	45.8	2.72 dd (9.6, 12.6) 3.02 dd (4.2, 12.6)		
11	14.5	0.98 s	12.5	0.44 d (6.6)		
12	17.2	1.59 s	19.6	1.15 s		
13	132.8	5.91 dd (10.2, 15.6)	132.3	5.94 dd (10.2, 15.6)		
14	133.9	5.64 ddd (6.0, 10.2, 15.6)	133.2	5.68 ddd (6.0, 10.2, 15.6)		
15	39.5	2.11 dd (6.0, 12.6) 2.54 m	39.0	2.10 dd (6.0, 12.0) 2.51 m		
16	42.9	3.38 dqd (1.8, 6.6, 11.4)	42.9	3.37 m		
17	216.9		217.0			
18	78.0		78.0			
19	61.4	3.44 d (2.4)	61.1	3.36 d (2.4)		
20	54.9	3.33 m	54.5	3.40 m		
21	73.9	5.73 s	74.1	5.54 s		
22	19.6	1.16 d (6.6)	19.7	1.16 d (6.6)		
23	22.4	1.51 s	22.3	1.51 s		
24	172.3		172.2			
25	20.6	2.19 s	20.6	2.14 s		
1'	139.1		138.3			
2'	129.9	7.31 m	131.2	7.29 m		
3'	130.9	7.33 m	129.8	7.29 m		
4'	128.0	7.23 m	128.7	7.23 m		
5'	130.9	7.33 m	129.8	7.29 m		
6'	129.9	7.31 m	131.2	7.29 m		

[a] Data were measured in CD_3OD at 600 MHz for ^1H and 150 MHz for ^{13}C.

2.3.8. 19,20-Epoxycytochalasin T (8)

Amorphous white powder. $[\alpha]_D^{26}$ = 114.6 (c 0.1, MeOH); UV (MeOH) λ_{max} (log ϵ) 325 (3.76) nm; IR (ZnSe) υ_{max} 3671, 3448, 2973, 1743, 1693, 1450, 1373, 1222, 1052, 1010 cm^{-1}; ^1H NMR and ^{13}C NMR data see Table 5; HRESIMS m/z 524.2643 $[M + H]^+$ (calcd. 524.2648 for $C_{30}H_{38}NO_7$).

2.3.9. (2R)-Butylitaconic acid (9)

Colorless needle crystal. $[\alpha]_D^{26}$ = −27.4 (c 0.1, MeOH); IR (ZnSe) υ_{max} 3400–2400, 1705, 1628, 1532, 1446, 1232, 1012, 953, 830 cm^{-1}; ^1H NMR and ^{13}C NMR data see Table 5; HRESIMS m/z 185.0815 $[M-H]^-$ (calcd. 185.0814 for $C_9H_{13}O_4$).

Table 4. IC_{50} values of compounds **1**, **5**, **7**, **10**, and **17** on nitric oxide production inhibitory activities induced by lipopolysaccharide in microglial BV-2 cells.

Compounds	IC_{50} (μM) [a]
1	19.55 ± 0.35
5	16.10 ± 0.57
7	15.20 ± 0.87
10	11.76 ± 0.49
17	11.30 ± 0.32
Curcumin	2.69 ± 0.34

[a] IC_{50} = concentration that reduces nitric oxide production by 50%.

Table 5. Anti-angiogenic activity of compounds **7**, **8**, and **21** in human endothelial progenitor cells.

Compounds	IC_{50} (μM) [a]
7	0.44 ± 0.01***
8	0.47 ± 0.03***
21	0.53 ± 0.01***
Sorafenib	5.50 ± 1.50

[a] Human endothelial progenitor cells were treated with the indicated compounds for 48 h. Anti-angiogenic activity was evaluated in a cell growth assay. Data are displayed as the mean ± SEM. Sorafenib, a well-known anti-angiogenic agent, was used as a positive control.

2.4. Sugar composition analysis of compounds **1**, **4**, and **5**

Compounds **1**, **4**, and **5** (each 2 mg) were heated at 90 °C with 4 M aqueous TFA (1 mL) for 3 h. After 2 mL of H_2O was added, the mixture was extracted with EtOAc (2 mL × 3). The H_2O layer was evaporated in vacuum to give a sugar fraction. The sugar fraction was analyzed and isolated by HPLC under the following conditions: column, SUPELCOSIL™ LC-NH2 (250 × 4.6 mm, 5 μm); mobile phase, acetonitrile/water (9:1, v/v); flow rate, 1.0 mL/min. Identification of D-glucose was carried out by comparison of the retention time and optical rotational value with those of authentic samples. D-glucose: t_R = 3.8 min; $[\alpha]_D^{26}$ + 52.5. The optical rotational values and ^{1}H NMR data of the aglycone parts of **1**, **4**, and **5** were listed below.

Compound ***1a****:* $[\alpha]_D^{26}$ = −15.2 (*c* 0.1, MeOH); ^{1}H NMR (600 MHz, $CDOD_3$): δ_H 7.02 (1H, s), 6.69 (1H, s), 4.33 (1H, m), 3.79 (3H, s), 1.28 (6H, m), 0.90 (3H, t, *J* = 7.2 Hz).

Compound ***4a****:* $[\alpha]_D^{26}$ = −49.8 (*c* 0.1, MeOH); ^{1}H NMR (600 MHz, $CDOD_3$): δ_H 7.03 (1H, d, *J* = 9.0 Hz), 6.71 (1H, d, *J* = 9.0 Hz), 4.70 (1H, m), 3.18 (1H, dd, *J* = 16.8, 6.0 Hz), 2.63 (1H, dd, *J* = 16.8, 11.4 Hz), and 1.51 (3H, s).

Compound ***5a****:* $[\alpha]_D^{26}$ = −24.0 (*c* 0.1, MeOH); ^{1}H NMR (600 MHz, $CDOD_3$): δ_H 7.53 (1H, d, *J* = 9.0 Hz), 6.85 (1H, d, *J* = 9.0 Hz), 4.73 (1H, m), 4.55 (2H, s), 3.22 (1H, dd, *J* = 16.8, 3.0 Hz), 2.85 (1H, dd, *J* = 16.8, 10.8 Hz), and 1.52 (3H, d, *J* = 6.6 Hz).

2.5. Preparation of the (S)- and (R)-MTPA esters of compounds 2 and 3

Compounds **2** and **3**, each was divided into two groups, and each was dissolved in 500 μL of pyridine-d_5. The pure compounds were then treated with 5 μL of (*S*)-α-methoxy-α-trifluoromethylphenylacetic chloride (MTPA-Cl) or 5 μL of (*R*)-MTPA-Cl at room temperature, and were stirred for 4h. The ^{1}H NMR spectra for (*S*)-Mosher esters (**2S** and **3S**) and (*R*)-Mosher esters (**2R** and **3R**) were recorded as below:

(S)-MTPA esters of 2 (2S): ^{1}H NMR (600 MHz, C_5D_5N): δ_H 6.04 (1H, d, *J* = 3.6 Hz), 5.91 (1H, dd, *J* = 11.4, 7.8 Hz), 5.74 (1H, d, *J* = 3.6 Hz), 5.27 (1H, dd, *J* = 18.6, 9.6 Hz), 3.68 (3H, s), 1.92 (2H, m), 1.77 (2H, m), and 1.28 (3H, d, *J* = 9.6 Hz).

(R)-MTPA esters of 2 (2R): ^{1}H NMR (600 MHz, C_5D_5N): δ_H 6.36 (1H, d, *J* = 3.6 Hz), 6.03 (1H, dd, *J* = 11.4, 7.8 Hz), 5.76 (1H, d, *J* = 3.6 Hz), 5.21 (1H, dd, *J* = 18.6, 9.6 Hz), 3.61 (3H, s), 2.12 (2H, m), 1.68 (2H, m), and 1.15 (3H, d, *J* = 9.6 Hz).

(S)-MTPA esters of 3 (3S): ^{1}H NMR (600 MHz, C_5D_5N): δ_H 6.51 (1H, d, *J* = 3.6 Hz), 5.67 (1H, d, *J* = 3.6 Hz), 4.80 (1H, dd, *J* = 11.4, 7.8 Hz), 4.08 (1H, dd, *J* = 18.0, 10.2 Hz), 3.63 (3H, s), 2.04 (2H, m), 1.89 (2H, m), and 1.35 (3H, d, *J* = 9.6 Hz).

(R)-MTPA esters of 3 (3R): ^{1}H NMR (600 MHz, C_5D_5N): δ_H 6.31 (1H, d, *J* = 3.6 Hz), 5.95 (1H, dd, *J* = 11.4, 7.8 Hz), 5.76 (1H, d, *J* = 3.6 Hz), 5.25 (1H, dd, *J* = 18.0, 10.2 Hz), 3.64 (3H, s), 1.96 (2H, m), 1.65 (2H, m), and 1.25 (3H, d, *J* = 9.6 Hz).

2.6. Single crystal X-ray diffraction analysis

Colorless needle crystals of compound **6** were obtained in methanol-dichloromethane-acetone (4:1:1). The data collection was carried out using Cu Kα radiation, and the crystal data and experimental details are listed in Tables S1 and S2 (https://doi.org/10.38212/2224-6614.3501). Crystallographic data for compound **6** have been deposited in the Cambridge Crystallographic Data Centre (CCDC) with number 2290180.

Crystallographic data for compound ***6****:* $C_{26}H_{40}O_9$ (M = 496.59), monoclinic crystal, space group *P*21, unit cell dimensions *a* = 12.9573 (4) Å, *b* = 6.4656 (2) Å, *c* = 15.2654 (5) Å, α = 90°, β = 91.0625 (13)°, γ = 90°, V = 1278.67 (7) $Å^3$, Z = 2,ρ_{calc} = 1.337 g/m^3, μ = 0.845 mm^{-1}. Flack parameter = 0.03 (5).

Colorless needle crystals of **7** were obtained in methanol-dichloromethane (2:1). The data collection was carried out using Cu Kα radiation, and the crystal data and experimental details are listed in Tables S3 and S4 (https://doi.org/10.38212/2224-6614.3501). Crystallographic data for compound **7** have been deposited in the Cambridge Crystallographic Data Centre (CCDC) with number 2290181.

Crystallographic data for compound ***7****:* $C_{30}H_{37}NO_7$ (M = 523.62), monoclinic crystal, space group *P*21, unit cell dimensions *a* = 13.1017 (11) Å, *b* = 7.0595 (6) Å, *c* = 15.8773 (14) Å, α = 90°, β = 93.773 (4)°, γ = 90°, V = 1465.3 (2) $Å^3$, Z = 2,ρ_{calc} = 1.228 g/m^3, μ = 0.727 mm^{-1}. Flack parameter = −0.04 (9).

2.7. Cell culture

The mouse BV-2 microglia cell line was cultured in DMEM supplemented with penicillin (90 units/mL), streptomycin (90 μg/mL), L-glutamine (3.65 mM), HEPES (18 mM), $NaHCO_3$ (23.57 mM), and 10% heat-inactivated fetal bovine serum (FBS) at 37 °C in a humidified atmosphere (95% O_2 and

5% CO_2). The cell culture conditions and treatments have been previously described [10].

2.8. MTT assay

Cell viability was measured using colorimetric MTT assay. In brief, BV-2 cells were seeded in 12-well plate at a density of 1×10^6 and incubated with various concentrations of all the pure isolates (20 μM) for 22.5 h. After treatment, MTT (0.55 mg/mL) was added and further incubated for 1.5 h. Then the cells were lysed in 1 mL DMSO. The absorbance values at 550 nm were measured on a microplate reader (Thermo Multiskan GO, Ratastie, Finland).

2.9. Measurement of nitric oxide production

Nitric oxide (NO) level in the culture supernatant was measured using nitrate/nitrite colorimetric assay kit (Cayman, Ann Arbor, MI, United States). BV-2 cells were seeded at a density of 1×10^6 in 12-well plate. After LPS-stimulation for 24 h in the presence or absence of all the pure isolates, the culture supernatants were collected to measure NO production. 100 μL culture supernatant was mixed with 50 μL Griess regent A and 50 μL Griess regent B sequentially and incubated for 20 min. Absorbance values at 550 nm were measured on a microplate reader (Thermo Multiskan GO, Ratastie, Finland) and nitrite concentrations were calculated by comparison to the nitrite standard.

2.10. Anti-angiogenesis assay

The protocols for cell culture of human endothelial progenitor cells (EPCs) have been described in detail previously [11]. The anti-angiogenic activities of selected compounds were evaluated by cell growth assay according to our previous method [12].

2.11. Statistical analysis

The results were obtained from three independent experiments and then presented as the mean ± standard deviations (SD). Graphpad Prism 6.0 software (GraphPad Software, San Diego, CA, USA) was used to analyze the data. One way ANOVA was used to compare the differences among the groups, and the Tukey method was used to make multiple comparisons of the means of the data in each group. Differences were considered significant at $*p < 0.05$, $**p < 0.01$, and $***p < 0.001$.

3. Results and discussion

In this study, the brown alga *S. cristaefolium*-derived fungal strain *X. acuta* SC1019 was cultured in liquid and solid media, and twenty-one compounds including nine previously undescribed compounds **1**−**9** (Fig. 1) along with twelve known compounds, PC-2 (**10**) [7], necpyrone C (**11**) [13], (1′*R*, 2′*S*)-LL-P880γ (**12**) [14], (*S*)-4-methoxy-6-pentanoyl-5,6-dihydro-2*H*-pyran-2-one (**13**) [15], LL-P880β (**14**) [16], (−)-epipestalotin (**15**) [17], (−)-pestalotin (**16**) [17], 5,6-dihydro-4-methoxy-6-(pentanoyloxy)-2*H*-pyran-2-one (**17**) [18], (*Z*)-3-methoxypent-2-enedioic acid (**18**) [19], (3*R*)-5-hydroxymellein (**19**) [20], 6-hydroxy-3-methyl-3,4-dihydroisocoumarin-5-carboxylic acid (**20**) [21], and cytochalasin C (**21**) [22], were identified from the extracts of the fermented products.

Compound **1** was obtained as white powder. The quasi-molecular ion peak $[M + H]^+$ at *m/z* 375.1651 (calcd. 375.1655 for $C_{17}H_{27}O_9$) in the HRESIMS and supported by ^{13}C NMR of **1** (Table 1) indicated a molecular formula of $C_{17}H_{26}O_9$. The IR spectrum indicated the presence of a hydroxy (3373 cm^{-1}) and a conjugated ester carbonyl (1691 cm^{-1}). The ^{1}H and ^{13}C NMR spectra of **1** revealed signals for an α-pyrone skeleton consistent with those of PC-2 (**10**), and the signals for the partial structure conjugated to the α-pyrone skeleton was assigned to be a sugar moiety including δ_H 4.81 (H-1′), 3.83 (H-6′a), 3.68 (H-3′ and -6′b), 3.67 (H-5′), 3.41 (H-2′), and 3.29 (H-4′); and δ_C 98.3 (C-1′), 74.9 (C-3′), 74.8 (C-5′), 73.4 (C-2′), 71.9 (C-4′), and 62.8 (C-6′) (Table 1). The HMBC correlations from H-7 to the anomeric carbon C-1′ suggested the sugar was attached at C-7. The mutually-coupled *J* values of $J_{H\text{-}1'/H\text{-}2'}$ (3.6 Hz), $J_{H\text{-}2'/H\text{-}3'}$ (9.6 Hz), $J_{H\text{-}3'/H\text{-}4'}$ (9.6 Hz), and $J_{H\text{-}4'/H\text{-}5'}$ (9.6 Hz) in the ^{1}H NMR spectrum of **1** indicated that the sugar moiety in **1** was an α-glucopyranose. Acid hydrolysis of **1** followed by HPLC purification afforded an α-pyrone aglycone **1a** and a glucose **1b**. The absolute configuration of C-7 in **1a** was assigned to be *S* form by comparing its optical rotational value $[\alpha]_D^{26}$ − 15.2 with $[\alpha]_D^{25}$ + 59.8 of PC-2 (**10**). The stereochemistry of **1b** was established to be D form by comparing the optical rotational value $[\alpha]_D^{26}$ + 37.6 with $[\alpha]_D^{26}$ + 52.5 of the authentic D-glucose. Thus, the structure of **1** was assigned as shown, and was named as xylarilactone A.

Compound **2** was deduced to have the molecular formula of $C_{11}H_{16}O_5$ established by a quasi-molecular ion $[M + H]^+$ *m/z* 229.1071 (calcd. 229.1076 for $C_{11}H_{17}O_5$) from HRESIMS. A hydroxy (3373 cm^{-1}) and a conjugated ester carbonyl (1688 cm^{-1}) were observed in the IR spectrum of **2**. The spectroscopic

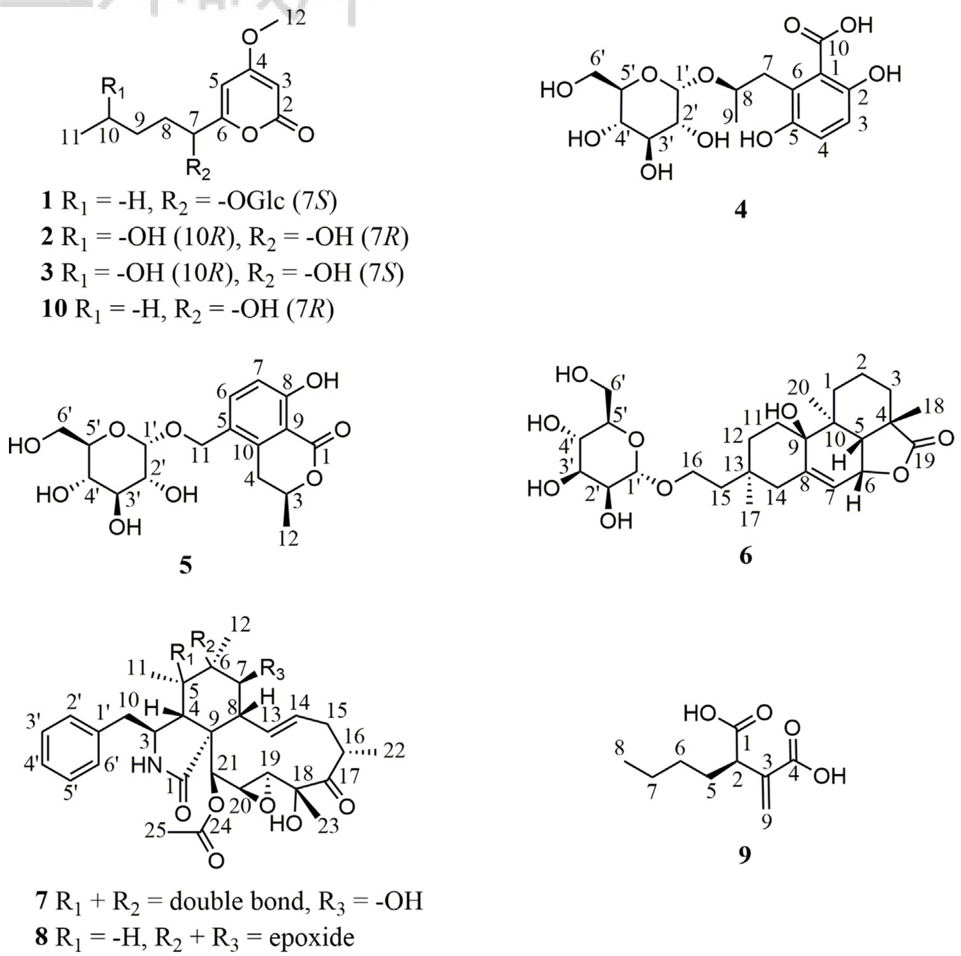

*Fig. 1. Chemical structures of compounds **1−10** isolated in this study.*

data of **2** were almost compatible with those of PC-2 (**10**) except that a methylene signal at δ_H 1.35 (2H, m, H_2-10) and δ_C 23.6 (C-10) in **10** were substituted by a carbinoyl methine signal at δ_H 3.74 (1H, dd, H-10)/δ_C 68.6 (C-10) (Table 1), respectively, in **2**, indicating a hydroxy group attached at C-10 based on a key cross-peak of H_3-11/H-10 in the COSY spectrum of **2**. The absolute configurations of C-7 and C-10 in **2** were determined by modified Mosher's method [23]. When **2** was reacted with (*R*)- and (*S*)-MTPA chloride to give the corresponding (*S*)- and (*R*)-MTPA esters **2S** and **2R**, respectively, the observed chemical shift differences $\Delta\delta_{S-R}$ values clearly established both *R* form configurations of C-7 and C-10 in **2** (Fig. 2).

Compound **3** was assigned the molecular formula $C_{11}H_{16}O_5$ from HRESIMS and supported by its ^{13}C NMR (Table 1). The UV and IR spectra of **3** were similar to those of **2**. The ^1H NMR data of **3** were almost compatible with those of **2** except a methylene H_2-8 signal at δ_H 1.96 and 1.68 in **2** shifted to δ_H 1.87 and 1.78, respectively, in **3** (Table 1), suggesting a diastereoisomer of **2**. The absolute configurations of C-10 and C-7 in **3** was deduced to be *R* and *S* forms, respectively, by application of the same modified Mosher's method (Fig. 2) as described above.

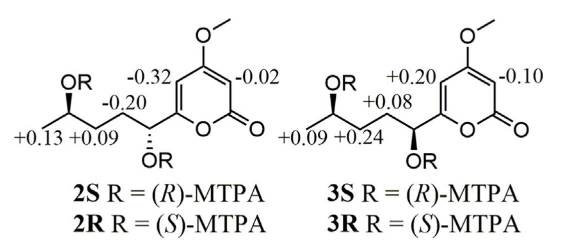

Fig. 2. $\Delta\delta_{S-R}$ values (in ppm) of ^1H NMR obtained from (S)- and (R)-MTPA esters of compounds 2 and 3 in pyridine-d_5 (600 MHz).

Compound **4** was obtained as amorphous white powder. The molecular formula was determined to be $C_{16}H_{22}O_{10}$ from the pseudo-molecular ion peak $[M-H_2O + H]^+$ at *m/z* 357.1175 (calcd. 357.1186 for $C_{16}H_{21}O_9$) in the HRESIMS. The IR spectrum indicated the presence of a hydroxy (3366 cm^{-1}), a conjugated acid carbonyl (1671 cm^{-1}), and an aromatic (1616, 1515, and 1473 cm^{-1}) functionalities. In the ^1H NMR spectrum (Table 2), an AX spin system signals at δ_H 7.50 (1H, d, $J = 9.0$ Hz, H-3) and 6.81 (1H, d, $J = 9.0$ Hz, H-4) as well as a methyl doublet at δ_H 1.52 (3H, d, $J = 6.0$ Hz, H-9) were observed. The ^1H NMR data of **4** also showed the presence of an α-glucopyranose moiety, for which the anomeric proton resonated at δ_H 5.34 (1H, d, $J = 3.6$ Hz, H-1′). The ^{13}C NMR and HSQC spectra revealed the presence of 16 carbon resonances, comprising one methyl, two methylenes, eight methines (two sp^2 and six sp^3), and four non-protonated carbons including a carboxylic acid group at δ_C 171.6 (C-10) (Table 2). From the COSY spectrum, a hexose moiety (H-1′ to H_2-6′) could be proposed (Fig. 3). The HMBC correlations from H-3 to C-1, -2, and -5, from H-4 to C-2, -5, and -6, from H-7 to C-1, -5, and -6, and from H-9 to C-7 and -8 indicated the presence of a phenolic acid moiety, which was linked to C-1′ by C-8 via oxygen as judged from the HMBC correlation between H-8 and C-1' (Fig. 3). Acid hydrolysis of **4** followed by HPLC purification gave an aglycone **4a** together with a D-glucopyranose ($[\alpha]_D^{26}$ + 38.4). The absolute configurations of C-8 in **4a** was assigned as *R* form by comparing its optical rotational value $[\alpha]_D^{26}$ − 49.8 with $[\alpha]_D^{25}$ + 23.4 of (*S*)-3,6-dihydroxy-2-(2-hydroxypropyl)benzoic acid in the literature [24].

Compound **5** was obtained as amorphous white powder, and had a molecular formula of $C_{17}H_{22}O_9$, as determined by HRESIMS at *m/z* 371.1335 $[M + H]^+$ (calcd. 371.1342 for $C_{17}H_{23}O_9$). The IR spectrum indicated the presence of a hydroxy (3365 cm^{-1}), a

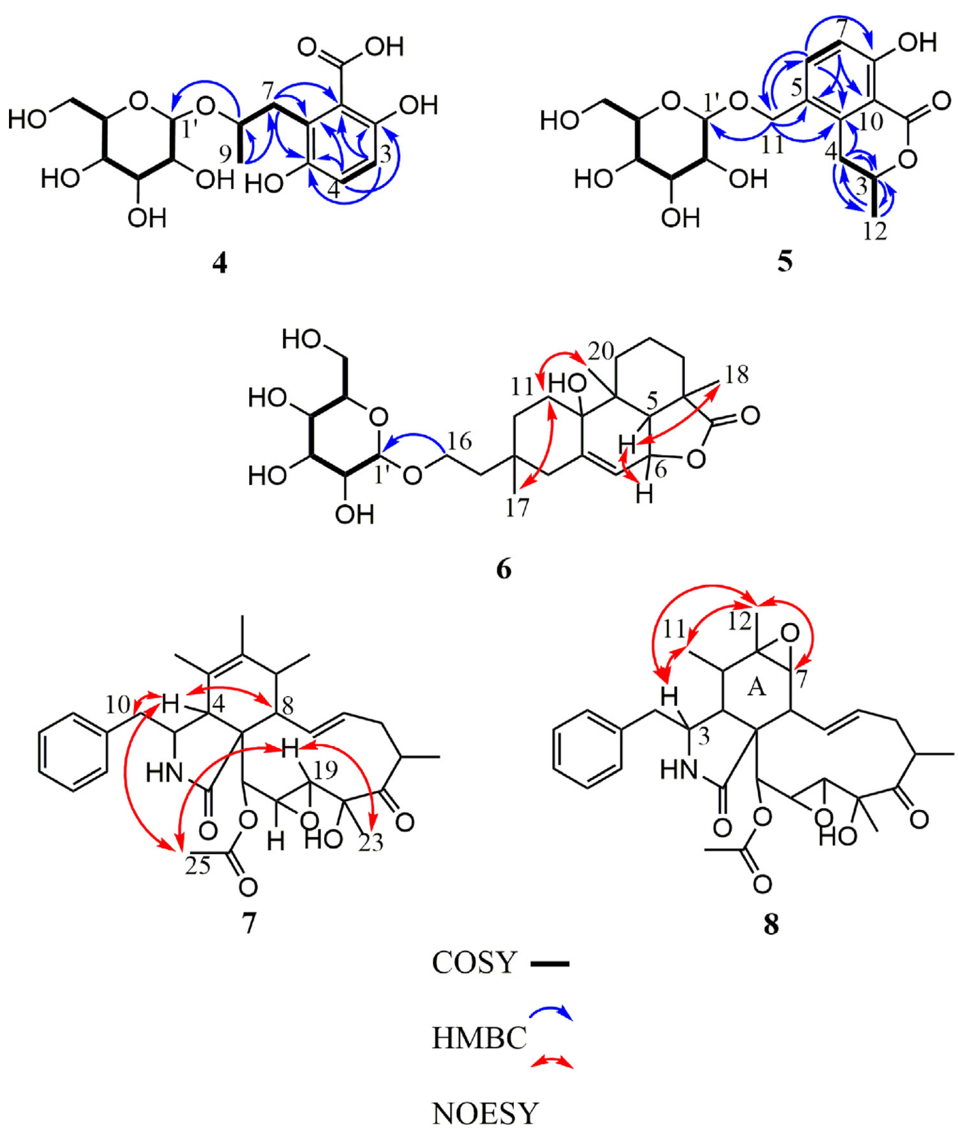

Fig. 3. Key COSY, HMBC, and NOESY correlations of compounds **4**–**8**.

conjugated carbonyl (1666 cm^{-1}), and an aromatic (1604 and 1475 cm^{-1}) functionalities. The ^{1}H NMR spectrum exhibited one 1,2,3,4-tetrasubstituted phenyl ring at δ_H 7.58 (1H, d, J = 8.4 Hz, H-6) and 6.84 (1H, d, J = 8.4 Hz, H-7), one methyl doublet at δ_H 1.52 (3H, d, J = 6.6 Hz, H-12), and an α-glucopyranose moiety, for which the anomeric proton resonated at δ_H 4.84 (1H, d, J = 3.6 Hz, H-1′) (Table 2). The ^{13}C NMR (Table 2) and HSQC spectra revealed the presence of 17 carbon resonances, including one methyl, three methylenes, eight methines (two sp^2 and six sp^3), and five non-protonated carbons. The HMBC correlations from H-3 to C-4 and -12, from H-4 to C-3, -10, and -12, from H-6 to C-8, -10 and -11, from H-7 to C-5 and -9, and from H-12 to -3, and -4 suggested an isocoumarin moiety, which was linked to C-1′ by C-11 via oxygen evidenced from the HMBC correlation between H-11 and C-1' (Fig. 3). Acid hydrolysis of **5** followed by HPLC purification afforded an isocoumarin moiety **5a** along with a D-glucopyranose ($[\alpha]_D^{26}$ + 41.0). The absolute configurations of C-3 in **5a** was determined to be *R* form by comparing its optical rotational value $[\alpha]_D^{26}$ − 24.0 with $[\alpha]_D^{20}$ − 105.0 of (*R*)-8-hydroxy-5-(hydroxymethyl)-3-methylisochroman-1-one [25].

Compound **6** was determined to have the molecular formula $C_{26}H_{40}O_9$ as deduced from a deprotonated molecular ion $[M-H]^-$ at *m/z* 495.2609 (calcd. 495.2594 for $C_{26}H_{39}O_9$) and a protonated molecular ion $[M + H]^+$ at *m/z* 497.2735 (calcd. 497.2751 for $C_{26}H_{41}O_9$) in the HRESIMS. The IR spectrum indicated the presence of a hydroxy (3367 cm^{-1}), a γ-lactone carbonyl (1747 cm^{-1}), and an aromatic (1596 and 1454 cm^{-1}) functionalities. The ^{1}H and ^{13}C NMR spectra of **6** revealed signals for a diterpene skeleton consistent with those of hymatoxin E [26], and the signals for the partial structure conjugated to the diterpene skeleton was assigned to be a sugar moiety including δ_H 4.73 (H-1′), 3.84 (H-6′a), 3.77 (H-2′), 3.71 (H-6′b), 3.67 (H-3′), 3.59 (H-4′), and 3.54 (H-5′); and δ_C 101.9 (C-1′), 75.0 (C-5′), 72.8 (C-3′), 72.4 (C-2′), 68.9 (C-4′), and 63.1 (C-6′) (Table 2). The HMBC correlations from H-16 to the anomeric carbon C-1′ indicated the sugar was attached at C-16 of the aglycone part of **6** (Fig. 3). The mutually-coupled J values of $J_{H\text{-}1'/H\text{-}2'}$ (1.8 Hz), $J_{H\text{-}2'/H\text{-}3'}$ (3.6 Hz), $J_{H\text{-}3'/H\text{-}4'}$ (9.6 Hz), and $J_{H\text{-}4'/H\text{-}5'}$ (9.6 Hz) in the ^{1}H NMR spectrum of **6** indicated that the sugar moiety in **6** was an α-mannopyranose [27,28]. The NOESY correlations of H_3-17/H-11α (δ_H 1.86) and H-11α (δ_H 1.86)/H_3-20 indicated that H-17, and H-20 were on the same side (Fig. 3), while the NOESY correlations of H-6/H-5 and H-5/H_3-18 indicated that H-6, -5, and H_3-18 were on opposite side. Furthermore, a single-crystal X-ray diffraction analysis of **6** was performed using the anomalous scattering of Cu Kα radiation (Fig. 4), which corroborated the absolute stereochemistry of **6** to be an *ent*-hymatoxin E coupled with an α-D-mannopyranose. Unambiguously, the structure of compound **6** was elucidated to be as shown, and was named as *ent*-hymatoxin E 16-*O*-α-D-mannopyranoside.

Compound **7** was obtained as white powder and gave a molecular formula of $C_{30}H_{37}NO_7$, as determined by HRESIMS at *m/z* 524.2626 $[M + H]^+$ (calcd. 524.2648 for $C_{30}H_{38}NO_7$). The IR spectrum indicated the presence of a hydroxy (3428 cm^{-1}), a γ-lactam (1700 cm^{-1}), and an ester carbonyl (1743 cm^{-1}). The ^{1}H NMR spectrum exhibited one monosubstituted phenyl ring [δ_H 7.33 (2H, m, H-2′ and H-6′), 7.31 (2H, m, H-3′ and H-5′), and 7.23 (1H, m, H-4′)], four singlet methyls [δ_H 2.19 (3H, s, H-25), 1.59 (3H, s, H-12), 1.51 (3H, s, H-23), and 0.98 (3H, s,

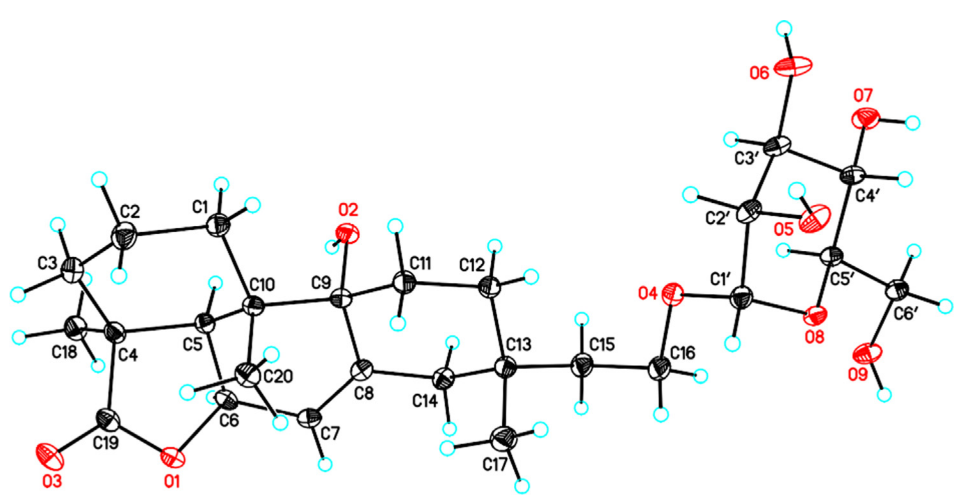

Fig. 4. Computer-generated perspective drawings of the X-ray crystallographic model of compound **6**.

H-11)], one doublet methyl [δ_H 1.16 (3H, d, J = 6.6 Hz, H-22)], and two olefinic methines [δ_H 5.91 (1H, dd, J = 15.6, 10.2 Hz, H-13) and 5.64 (1H, ddd, J = 15.6, 10.2, 6.0 Hz, H-14)] (Table 3). The ^{13}C NMR and HSQC spectra revealed the presence of 30 carbon resonances, comprising five methyls, two methylenes, fifteen methines, and eight quaternary carbons (Table 3). The NMR spectrum data of 7 closely correlated with those of 19,20-epoxycytochalasin C [4], except that the $\delta_{H\text{-}11}$ 1.43 in 19,20-epoxycytochalasin C upfield shifted conspicuously to $\delta_{H\text{-}11}$ 0.98 in 7, suggesting some chemical environmental differences around H_3-11 between 19,20-epoxycytochalasin C and 7. Further assignments of COSY, HSQC, and HMBC spectra revealed that 7 had the same plain structure as that of 19,20-epoxycytochalasin C, indicating 7 was a diastereoisomer of 19,20-epoxycytochalasin C. The NOESY correlations of H_3-23/H-19, H-19/H_3-25, H_3-25/H-4, and H-4/H-8 and -10 indicated that H_3-25, H_3-23, H-19, H_2-10, H-8, and H-4 were on the same side (Fig. 3). No vicinal cross-peak between H-3 and H-4 was observed in the NOESY spectrum, suggesting H-3 and H-4 were *trans*-oriented. A single-crystal X-ray diffraction analysis of 7 was performed using the anomalous scattering of Cu Kα radiation (Fig. 5), which corroborated the absolute configuration of 7 as C-4 epimer of 19,20-epoxycytochalasin C. In comparison with $\delta_{H\text{-}11}$ value of 19,20-epoxycytochalasin C, the obvious upfield shift of olefinic H_3-11 in 7 was speculated to be resulted from diamagnetic ring current effect of a benzene ring based on ChemBio 3D Ultra 12.0 molecular modelling (Fig. S82) (https://doi.org/10.38212/2224-6614.3501).

Compound 8 was obtained as white powder, and gave a molecular formula of $C_{30}H_{37}NO_7$, as determined by HRESIMS at m/z 524.2643 $[M + H]^+$ (calcd. 524.2648 for $C_{30}H_{38}NO_7$). The IR spectrum indicated the presence of a hydroxy (3448 cm^{-1}), a γ-lactam (1693 cm^{-1}), and an ester carbonyl (1743 cm^{-1}) functionalities. The spectroscopic data of 8 were almost compatible with those of 7 except that a methyl signal at δ_H 0.98 (3H, s, H_3-11)/δ_C 14.5 (C-11), a double bond signal at δ_C 128.1 (C-5) and 134.0 (C-6), and a carbinoyl methine signal at δ_H 3.73 (1H, dd, J = 1.2, 10.2 Hz, H-7)/δ_C 70.2 (C-7) in the ^1H and ^{13}C NMR spectra of 7 were substituted by a methyl signal at δ_H 0.44 (3H, d, J = 6.6 Hz, H-11), a methine signal at δ_H 1.48 (1H, m, H-5), and an epoxide signal at δ_C 56.6 (C-6) and δ_H 2.65 (1H, d, J = 5.4 Hz, H-7)/δ_C 64.3 (C-7) in those of 8, respectively. Comprehensive analysis of the 1D (Table 3) and 2D NMR data allowed for the establishment of the plain structure of 8, which was the same as that of 19,20-epoxycytochalasin Q [4]. Based on biogenetic relationship in the same fungal strain, compound 8 was assigned to adopt the same absolute configurations with those of 7 except that some structural changes at A ring of 8, especially for its C-5−C-7. In the NOESY spectrum, key cross-peaks of H_3-12/H_3-11, H-7, and -3 and H_3-11/H-3 indicated that H_3-12, -11, and H-7 and -3 were on the same side (Fig. 3). No correlation between H-3 and H-4 was observed in the NOESY spectrum, suggesting vicinal H-3 and H-4 would be oriented on different side. Thus, the structure of 8 was assigned to be C-4 epimer of 19,20-epoxycytochalasin Q as shown, and was named 19,20-epoxycytochalasin T.

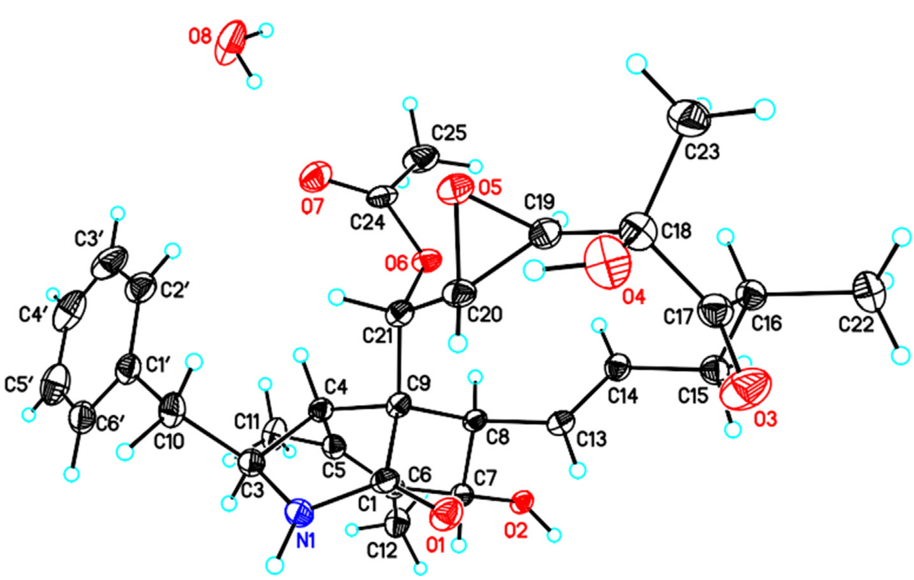

Fig. 5. Computer-generated perspective drawings of the X-ray crystallographic model of compound 7.

The HRESIMS of compound **9** showed a deprotonated $[M-H]^-$ peak at *m/z* 185.0815 (calcd. 185.0814 for $C_9H_{13}O_4$), indicating a molecular formula of $C_9H_{14}O_4$. The IR spectrum indicated the presence of a carboxylic acid (3400−2400 and 1705 cm^{-1}). The ^{13}C NMR and HSQC spectra revealed the presence of nine carbon resonances, comprising one methyl, four methylenes, one methine, and three non-protonated carbons (Table 3). The correlations observed in COSY, HSQC, and HMBC spectra showed that **9** had the same gross structure as (2*S*)-butylitaconic acid [29]. The absolute configuration of the only asymmetric C-2 in **9** was deduced to be *R* form by comparing its specific optical rotational value $[\alpha]_D^{26} - 27.4$ with $[\alpha]_D^{22} + 10.3$ of (2*S*)-butylitaconic acid.

All the isolates **1−21** were assessed for anti-neuroinflammatory and anti-angiogenesis activities. Before conducting the anti-neuroinflammatory assay, the MTT method was employed to evaluate the cytotoxic effects of these compounds on BV-2 cells. This preliminary evaluation aimed to prevent any potential impact on nitric oxide (NO) release arising from compromised cell viability. All test compounds didn't exert any significant cytotoxicity at a concentration of 20 μM (Fig. S81) (https://doi.org/10.38212/2224-6614.3501). The IC_{50} values of compounds **1**, **5**, **7**, **10**, and **17** on NO production inhibitory activities in lipopolysaccharide-activated BV-2 microglial cells were further determined to be 19.55 ± 0.35, 16.10 ± 0.57, 15.20 ± 0.87, 11.76 ± 0.49, and 11.39 ± 0.32 μM (Table 4), respectively. The anti-angiogenesis activity was evaluated in human endothelial progenitor cells (EPCs), and compounds **7**, **8**, and **21** exhibited inhibitory effects of EPCs growth with IC_{50} values of 0.44 ± 0.01, 0.47 ± 0.03, and 0.53 ± 0.01 μM (Table 5), respectively.

Conflicts of interest

The authors declare no competing financial interest.

Acknowledgments

We thank Ms. S. -Y. S. and Ms. A. G. in the Instrumentation Center of the College of Science, National Taiwan University and the Instrumentation Center of Taipei Medical University for the MS and NMR data acquisition, respectively. This work was supported by a grant from the National Science and Technology Council (MOST 110-2320-B-002-023-MY3) of Taiwan to T. -H. L.

References

[1] Chen JJ, Wang SW, Chiang YR, Pang KL, Kuo YH, Shih TY, et al. Highly oxygenated constituents from a marine alga-derived fungus *Aspergillus giganteus* NTU967. Mar Drugs 2020;18:303.
[2] Hsiao G, Wang SW, Chiang YR, Chi WC, Kuo YH, Phong DA, et al. Anti-inflammatory effects of peptides from a marine algicolous fungus *Acremonium* sp. NTU492 in BV-2 microglial cells. J Food Drug Anal 2020;28:89−97.
[3] Kirk PM, Cannon PF, David JC, Stalpers JA. Dictionary of the fungi 10th ed. Oxfordshire. 2008.
[4] Abate D, Abraham WR, Meyer H. Cytochalasins and phytotoxins from the fungus *Xylaria obovata*. Phytochemistry 1997;44:443−1448.
[5] Song F, Wu SH, Zhai YZ, Xuan QC, Wang T. Secondary metabolites from the genus *Xylaria* and their bioactivities. Chem Biodivers 2014;11:673−94.
[6] El-Beih AA, Kato H, Ohta T, Tsukamoto S. (3R, 4aR, 5S, 6R)-6-Hydroxy-5-methylramulosin: a new ramulosin derivative from a marine-derived sterile mycelium. Chem Pharm Bull 2007;55:953−4.
[7] Evidente A, Zonno MC, Andolfi A, Troise C, Cimmino A, Vurro M. Phytotoxic α-pyrones produced by *Pestalotiopsis guepinii*, the causal agent of hazelnut twig blight. J Antibiot 2012;65:203−6.
[8] Zheng N, Yao FH, Liang XF, Liu Q, Xu WF, Liang Y, et al. A new phthalide from the endophytic fungus *Xylaria* sp. GDG-102. Nat Prod Res 2018;32:755−60.
[9] Wu SH, Chen YW, Miao CP. Secondary metabolites of endophytic fungus *Xylaria* sp. YC−10 of *Azadirachta indica*. Chem Nat Compd 2011;47:858−61.
[10] Wang CH, Hsiao CJ, Lin YN, Wu JW, Kuo YC, Lee CK, et al. Carbamazepine attenuates inducible nitric oxide synthase expression through Akt inhibition in activated microglial cells. Pharm Biol 2014;52:1451−9.
[11] Lee MS, Wang SW, Wang GJ, Pang KL, Lee CK, Kuo YH, et al. Angiogenesis inhibitors and anti-inflammatory agents from *Phoma* sp. NTOU4195. J Nat Prod 2016;79:2983−90.
[12] Lee TH, Hsieh CL, Wu HC, Wang SW, Yu CL, Hsiao G, et al. Anti-lymphangiogenic diterpenes from the bark of *Calocedrus macrolepis var. formosana*. J Food Drug Anal 2021;29: 606−21.
[13] Li W, Li XB, Li L, Li RJ, Lou HX. α-Pyrone derivatives from the endolichenic fungus *Nectria sp*. Phytochem Lett 2015;12: 22−6.
[14] Le VT, Bertrand S, Robiou du Pont T, Fleury F, Caroff N, Bourgeade-Delmas S, et al. Untargeted metabolomics approach for the discovery of environment-related pyran-2-ones chemodiversity in a marine-sourced *penicillium restrictum*. Mar Drugs 2021;19:378.
[15] Strunz GM, Heissner CJ, Kakushima M, Stillwell MA. Metabolites of an unidentified fungus: a new 5, 6-dihydro-2-pyrone related to pestalotin. Can J Chem 1974;52:825−6.
[16] Kirihata M, Ohta K, Ichimoto I, Ueda H. Total synthesis of (6S, 1'S, 2'R)-6-(1', 2'-dihydroxypentyl)-4-methoxy-5, 6-dihydropyrane-2-one (LL-P880β) and its C6-epimer, a fungal metabolite from *Penicillium sp*. Agric Biol Chem 1990;54: 2401−5.
[17] Moriyama M, Nakata K, Fujiwara T, Tanabe Y. Divergent asymmetric total synthesis of all four Pestalotin diastereomers from (*R*)-Glycidol. Molecules 2020;25:394.
[18] Takesako K, Saito H, Ueno M, Awazu N, Kato I. U.S. Patent No. 6,261,826. Washington, DC. U.S. Patent and Trademark Office; 2001.
[19] Cornaggia C, Gundala S, Manoni F, Gopalasetty N, Connon SJ. Catalytic formal cycloadditions between anhydrides and ketones: excellent enantio and diastereocontrol, controllable decarboxylation and the formation of adjacent quaternary stereocentres. Org Biomol Chem 2016; 14:3040−6.
[20] Zhao L, Kim JC, Paik MJ, Lee W, Hur JS. A multifunctional and possible skin UV protectant, (3*R*)-5-hydroxymellein,

produced by an endolichenic fungus isolated from *Parmotrema austrosinense*. Molecules 2016;22:26.
[21] Zhang XQ, Qu HR, Bao SS, Deng ZS, Guo ZY. Secondary metabolites from the endophytic fungus *Xylariales* sp. and their antimicrobial activity. Chem Nat Compd 2020;56: 530−2.
[22] Edwards RL, Maitland DJ, Whalley AJ. Metabolites of the higher fungi. Part 24. Cytochalasin N, O, P, Q, and R. New cytochalasins from the fungus Hypoxylon terricola Mill. J Chem Soc Perkin Trans 1989;1:57−65.
[23] Su BN, Park EJ, Mbwambo ZH, Santarsiero BD, Mesecar AD, Fong HH, et al. New chemical constituents of *Euphorbia quinquecostata* and absolute configuration assignment by a convenient mosher ester procedure carried out in NMR tubes. J Nat Prod 2002;65:1278−82.
[24] Nguyen HX, Nguyen LT, Van Do TN, Le TH, Dang PH, Tran HM, et al. A new phenolic acid from the wood of *Mangifera gedebe*. Nat Prod Res 2021;35:2579−82.
[25] Okuno T, Oikawa S, Goto T, Sawai K, Shirahama H, Matsumoto T. Structures and phytotoxicity of metabolites from *Valsa ceratosperma*. Agric Biol Chem 1986; 50:997−1001.
[26] Borgschulte K, Rebuffat S, Trowitzsch-Kienast W, Schomburg D, Pinon J, Bodo B. Isolation and structure elucidation of hymatoxins B-E and other phytotoxins from *Hypoxylon mammatum* fungal pathogen of leuce poplars. Tetrahedron 1991;47:8351−60.
[27] Rivera-Chávez J, Figueroa M, González MDC, Glenn AE, Mata R. α-Glucosidase inhibitors from a *Xylaria feejeensis* associated with *Hintonia latiflora*. J Nat Prod 2015;78: 730−5.
[28] Nifant'ev NE, Shashkov AS, Lipkind GM, Kochetkov NK. Synthesis and ^{13}C NMR spectra of 2,3-di-*O*-glycosyl derivatives of methyl alpha-L-rhamnopyranoside and methyl alpha-D-mannopyranoside. Carbohydr Res 1992;237: 95−113.
[29] Li G, Kusari S, Lamshoft M, Schuffler A, Laatsch H, Spiteller M. Antibacterial secondary metabolites from an endophytic fungus, *Eupenicillium* sp. LG41. J Nat Prod 2014;77: 2335−41.